Meteorological Aspects in Storm Surge Modeling

Jye Chen
National Weather Service
NOAA

Abstract

The discussion has tried to focus on the elements of meteorological forcing to storm surge modeling. The difference of tropical and extra-tropical cyclones in the dynamical aspects as regard to storm surge modeling is compared. Specific experiments for storm surge computations are presented to illustrate the impact of the various kinds of meteorological forcing. The weak link of surge modeling to tropical cyclone predictions is specially analyzed.

1. Introduction

Apart from the daily astronomical tides, there are two types of weather events that generate additional water level changes, referred as storm surge, or sub-tidal water level: mid-latitude extra-tropical cyclones (EC) and tropical cyclones (TC). The prediction of astronomical tide at a tide gage can be made very accurately, sometimes to a few centimeter where the gage record is long. But, even the skill in predicting storm surge has been improved greatly along with the advancement of weather forecasting, and the numerical models have replaced the statistical methods, the accuracy is no match with astronomical tide prediction.

The reason is due to the definition of the surface wind and pressure, the primary forcing for storm surge generation. Today, the extra-tropical cyclone's development, EC cyclogenesis, can be very skillfully predicted by Numerical Prediction Model (NWP), evidenced by many recent events in the U.S. East Coast. The storm surge predictions also show their consistency with the NWP's skills. They will be illustrated here. The prediction can be put in the routine basics as NWP's operation. The lessons learned are very informative to the surge modeling problems.

The study of the TC dynamics and the track predictions have progressed significant in the past two decades. Only recently, the track prediction by dynamic models started showing promises for future advancement. A 24-hr forecast of TC's position has a RMS error of slightly under 100 NM, by many models, today. However, the demand of high precision in the location of the tight, strong wind band **near landfall** of TC makes the surge forecasting very difficult, so is applied to intensity. Consequently, the methodology for TC's surge prediction must follow that of TC forecast operation. This trend will continue.

In the past, the engineering tools are invented; the TC is described by an analytic formula with a set of simple parameters, called parametric wind model. In the hindcast mode, the surge model has shown its capability to reproduce the observed surges, even quantitatively. The accuracy is by no means comparable to EC's surge verification. For TC, even post-storm verification can not rectify the errors from the contributing factors: meteorology input, or ocean dynamics, or observations, or all of them. In U.S.'s East Coast and Gulf coast, significant TC surges are in the mean of 3 m, while EC surges are 1 m. The error in EC surge forecasts verified at a gage is of order of 10 to 15 cm; the error of post-storm verification for TC is only in 20 %.

The forecasting constraint on TC is so great that one tends to use the 'least regret' forecast in real time for the general public. We may also use surge model as an assessment tool for likelihood forecasts, or the worst and best scenario forecasts. The sensitivity study of surge model with respect to a large set of hypothetical situations can be helpful for the evacuation decision and other environmental analyses.

2. Oceanic Response: bathymetry and coastal geometry

The surge characteristics are complicated by coastline geometry and basin depths (bathymetry). Even a simple open continental shelf and a deep ocean respond to the forcing significantly different. In the deep ocean, because of the large 'external' Rossby radius of deformation, $\lambda_e = (gD)^{1/2}/f$, the cyclone's momentum generates mostly currents and internal (baroclinic) waves, excluding surface waves. The water levels, an external mode of motion is, hard to be excited.. On the shelf where responsible for storms surge generation, the barotropic mode dominates. A relative small baroclinic response from TC can last weeks in its wake, since the 'internal' Rossby radius of deformation, $\lambda_i = (\delta\rho/\rho)\lambda_e$, is small. Its effect do not penetrate into the shelf as illustrated by a two-layer ocean model (Bunpapong, et al 1985 for Gulf of Mexico). The storm surge on the open shelf is generated by two kinds of forcing: cross-shelf wind and long-shore wind. The forced convergence of transports induced by cross-shore wind onto the sloping depths and against the coasts is typical for the TC storms. The surge is transient, lasts normally less than a tidal cycle. Severe EC cyclones, northeasters in the East coast, are large, slowly moving systems; on-shore surge gradients are nearly in balance with long-shore currents. Their coastal impact is characterized by the long duration, surges coinciding with the astronomical high tide, and large waves.

For a semi-enclosed shelf comparable to the size of a cyclone, such as Yellow and Bohai seas in Asia; or, a wide strait between Taiwan and mainland continent, the storm surge distributions are complicated by lateral geometry and depths. Post-storm re-surges are common due to reflections, as free oscillations, such as edge waves, coastal trapped waves, natural mode of oscillations for semi-enclosed, or bays and estuaries coupling, etc.. They may also interact with the wind-induced direct surges (Qin,1993).

3. Extra-tropical Cyclones: lessons learned

Today's storm surge model for EC directly uses the lowest level wind and pressure from the numerical weather prediction (NWP) model, due to its high vertical resolution capability. The development of unstable baroclinic waves, as EC cyclogenesis (EC's 'cold-core' structure, in contrast with TC's warm-core) has been well reproduced by NWP. The EC's cold-core structure is characterized by strong vertical wind shear (thermal gradient), strong surface

pressure gradients and winds behind the cold front. The scale of EC is in the order of 1000 km; the typical life cycles of EC are several days to a week. The progress of forecasting U.S. Atlantic coastal EC cyclogenesis are very noticeable in many major events of recent years (e.g., super storm in March 1993).

3a. A quasi-stationary case: 1991's Halloween storm

See Fig. 1 for the bathymetry and computation grids for a operational EC's surge model for East Coast of U.S. (Chen, et al. 1993; Kim, et al. 1995). It uses the global operational model (AVN) output winds (.995 sigma level, roughly 30 m above MSL) (90 % values for sea surface) and surface pressure, in 1 degree resolution (from 126 spectral modes), (Fig. 2). This storm was initially merged with a TC in the Atlantic, then drifted westward and battered the coast. After three and half days, EC repacked the convective energy and turned into TC, made a loop and moved NE to Canada. The wind field contracted and left weaker wind on the shelf. Fig. 3 shows the hindcasted surge histories as compared with tidal gages data. The slow rise and the sharp drop of surge are well reproduced by surge model. Throughout the event, this region were dominated by N to NE winds; majority of the coasts experienced steady off-shore and slightly long-shore winds. It is worth to notice that in this case the **local winds** at a coastal point do not correlate to the local surges (Fig. 4), at Montauk, N.Y. The computed surges responded according to the storm's structure changes at the outer mid-Atlantic shelf.

3b. A transient case

The rapid EC cyclogenesis developed in 18 hour was in the forecast (Fig. 5). The surge forecasts in three consecutive forecast cycles showed consistencies in amplitudes and phases as the observed, credited to the NWP's forecasts. The coastal low pressure developments are common phenomena in the East Coasts, normally exiting to sea or along the coasts. Winds are transient easterly, in contrast with north-easterly for case 3a. Sometimes, the predictions suffer more from the temporal interpolations of the field variables.

3c. An approaching low center from ocean

This case is similar to TC's prediction. The surge forecasts are shown in Fig. 6. The forecasts of first two cycles, from 22/00Z and 22/12Z of Dec 1994, failed to produce the phase, because the storms were predicted too close to the coast. But, at 23/12Z, the model made a final correction for a useful 24-hr forecast. In this case, both time and space interpolations are crucial.

Using the saved analyzed wind/pressure fields (12 hr cycles) for two days, the initial state of ocean is produced by the model spin-up and warm-up from a no-motion state. Closer intervals than 12 hours are desirable (important for transient cases), but not implemented at this time. No true data assimilation is used for the initial state. Then, the model provides 48 hours surge forecasts along with NWP. This process repeats twice daily at 00Z and 12Z in a routine bases. The statistics for the 24 hr forecasts, in 1994, with the sub-tidal water level analyses at the gages have shown a root mean square error of 10-15 cm on the East Coast gages, and a correlation coefficient around .8.

The initial water levels at each coastal gage may contain variations in longer periods, such as seasonal change. Since they vary from location to location, a simple barotropic surge model can not reproduce such variations by spin-up from rest. In practice, local users can make such an adjustment by removing monthly mean from the real-time gage data.

4. Tropical cyclones: area of difficulties

For TC surge predictions, the greatest difficulty is predicting the storm, the motion and intensity. It is the problem of storm forecast, unanswered by surge models. Although the surge modeling effort has a long history on EC (over 40 years in Europe), it can not extend the experience to deal with TC meteorology. This is the weakest link of TC surge prediction to meteorology. In U.S., dynamical surge model was applied first for TC then later for EC; modeling the storm for TC has been the primary concern, with very little help from NWP's advancements.

4a. The primary and secondary circulation

In a mature TC, the primary circulation, the tangential winds, is highly symmetrical near the core region. The deep, lower-troposphere circulation is close to barotropic, in contrast to upper troposphere, where heating is take place, being baroclinc. This TC structure is by no means close to EC, a baroclinc wave. The difference lies on the secondary circulation being the primary role in supporting TC .

From RECON data, the cyclonic (northern hemisphere) primary flow can be shown in good gradient balance with pressure (Willoughby, 1990b). It is derived from measured geopotential heights on an isobaric surface (e.g.,700 or 850 mb flight level). The Minimum central Sea-Level Pressure (MSLP) measured by dropsonde is considered the best indicator for TC intensity; or by the 700 mb center height which is highly correlated with MSLP (Weatherford and Gray, 1988a). A maximum wind band around the center is nearly in cyclostrophic balance. These are practical elements of TC, used widely and only measured directly by RECON.

Without RECON, either MSLP and maximum wind is rarely measured by surface observations. Engineers must develop by empirical means the relationship for pressure and wind: 1. Analytic pressure profiles (Schloemer 1954, Myers 1954, Holland 1980); 2. Analytic wind profile (Jelesnianski and Taylor, 1973), JT, depending on a few empirical parameters. To close the formulas, the direct relation of peak wind speed and MSLP, WPR, is made by empirical means:

$$V_m = \text{const.}\ (p_\infty - p_o)^\alpha \qquad (1)$$

where V_m is the maximum wind, p_o is MSLP, p_∞ the pressure at large distance (α = .644, Atkinson and Holliday 1977). As α = 1/2, V_m is related to V_c, a cyclostrophic wind in the core. Or, V_m can be further adjusted to account for the latitude effect, as gradient wind, V_g, by

$$V_g = V_c / [\,(1 + a^2)^{1/2} + a\,] \qquad (2)$$

$$a = .5\,(f R_m)/ V_c$$

where f is the Coriolis parameter, R_m the radius of maximum wind. V_g near R_m is about 2 m/s lower than V_c. Their mathematical form of pressure profile is normalized by p_∞-p_o.

$$p - p_o = (p_\infty - p_o)\, P(x) \qquad (3)$$

and $x=r/R_m$, R_m the horizontal scale. For surface wind, a reduction factor (frequently .8, or .7) and a constant inflow angle (e.g. 25 degree) are frequently chosen.

The secondary circulation of TC, mainly vertical, is in response to condensation heating in the convective ring which is assumed under the control of frictional induced convergence. For a given primary circulation of a steady-state TC, the radial mean flow in the boundary layer, u, can be related to frictional dissipation and radial transports of absolute vorticity,

$$u = - C_D V_o^2 / h[\, r^{-1}(d/dr)\, Vr + f\,] \qquad (4)$$

where V_o is surface wind of V, h thickness of the boundary layer, C_D the drag coefficient. That $u<0$ inward, for all r outside the core region, since the bracket term is always positive for inertial stability. Typically, $V\sim r^{-x}$, $x\sim.5$; it results that, letting $V_o=V$, an inflow gradually increases from far distance inward to a maximum (at ~ 3 R_m if $f R_m/V_m=.2$) then drops toward center to zero. However, from (4), u is very sensitive to h.

Account for the radial flow, it can be derived from JT's formulation that the maximum **surface** wind and central pressure relationship, along a surface trajectory with a inflow angle $\phi(r)>0$ is

$$p_\infty - p_o = \rho V_m^2 k_s\, c \qquad (5)$$

$$c = \int_o^\infty f(x)^2\, [\sin\phi(r)]^{-1}\, dr$$

$$k_s \propto R_m^{1/2}/(.3\, V_m + 60)^{1/2},$$

R_m in mi, V_m in mph,

where the normalized wind **speed** formula $f(x)=2x/(1+x^2)$, $x=r/R_m$, k_s an empirical frictional constant which has no direct physical meaning, but adjusted to fit the data. The $\phi(r)$ and p(r), not known, are solved separately (see reference). As a result, c is a rather mild function of R_m, a dissipation measure along the trajectory. Larger storms have larger inflow angles at a distance; vice versa. See Fig. 7 for a range of R_m.

$$V_m = \text{const.}\, (p_\infty - p_o)^{1/2}\, R_m^{-1/4}\, c^{-1/2}\, (.3\, V_m + 60)^{1/4} \qquad (6)$$

In addition, the maximum surface wind speed is a mild function of radius of maximum wind. From an independent study (Chen, 1997), the parametric wind model by (Holland, 1980) can be extended to have a similar result as JT, if Holland's parameter B, is set , by fitting, to

$$B = 1.5\, (R_m/30)^{-1/2}\ ,\ R_m \text{ in mi} \qquad (7)$$

then,

$$V_c = \text{const.}\, (p_\infty - p_o)^{1/2}\, R_m^{-1/4} \qquad (8)$$

According Holland,, $1<B<2.5$, a mean of B is 1.5. Schloemer and Myers formulas, B=1, generally underestimate V_m. Their comparison is shown in Fig. 8. These refinement of WPR is realistic, according to data analysis of (Weatherford and Gray 1988a). In addition, JT's is capable to produce a realistic surface trajectory for a given central pressure, requiring no knowledge of maximum wind. This preference certainly has something to do with the availability of dropsonde data at the storm center from RECON.

The air-sea interaction theory of a steady-state TC (Emanuel, 1986) can quantitatively relate the central pressure and moist entropy, with the aid of gradient wind relationship for radial distribution of TC angular momentum at the top of boundary layer. The emphasis of the boundary layer thermal budget has been revealed in the numerical model experiment at TC's mature state (Ooyama, 1969). Ignoring horizontal diffusion, the angular momentum budget in the converging boundary layer (thickness h) can be derived as:

$$h\, r^{-1}\, (d/dr)[\, M u r\,] = - C_D |V_o| V_o - w_h M_h \qquad (9)$$

$$w_h = - h\, r^{-1}\, (d/dr)[\, u r\,] \qquad (10)$$

where M, $Vr + fr^2/2$, is the mean absolute angular momentum, u the mean radial velocity, $|V|=(V^2+u^2)^{1/2}$, w vertical velocity, subscripts o and h indicate $z=0$ and $z=h$, C_D the drag coefficient. The vertical mass flux, w_h, is positive (upward) at the cloud base, negative (subsidence) away from the core. This equation relates the inward increase of the tangential winds (angular momentum) toward the core against the frictional dissipation, downward mixing of momentum flux. Eliminating w_h, with $M_h=M$, (9) and (10) can be reduced to

$$h\, u\, [r^{-1}\, (d/dr)\, M] = - C_D |V_o| V_o\,,$$

the equation (4). Independently, from JT's formulation (see reference), it can be derived that for all **surface variables**

$$u_o[r^{-1}\, (d/dr)\, M_o] = - (k_s |V_o| V_o - k_n |V_o|\, u_o) \qquad (11)$$

where k_n is a constant in normal direction of the trajectory, as k_s the tangential, and $k_n = k_s/1.15$. Two empirical constants, no claim to be related to drag coefficient C_D, serve to fit the data only (Jelesnianski, 1966).

Emanuel's approach uses the gradient wind constraint at the top the boundary layer to predict, at the center of TC, the pressure and θ_E, equivalent potential temperature (representing moist entrophy). This thermal constraint to angular momentum leads to the prediction of intensity measure of TC as parameter of sea surface temperature T_s, cloud out-flow temperature T_{out} and boundary layer relative humidity in the outer core regions. The maximum wind and wind profile are also predicted at the top of boundary layer, so is WPR. This method may be useful, if the central pressure measurement is not available.

In reality, intense TCs frequently possess double concentric eye structures. They seem to also follow gradient balance (Willougby, et al. 1982). It is very easy to generalize JT's normalized wind profile, f(x), Fig. 9, to fit a wind profile of double maxima for hurricane Allen, 1980. Being consistent with pressure drop (also change of inflow angles) , the resulting surface wind speeds are quite reasonable, roughly 80% of flight-level winds. Both single-maximum profiles, R_m=12 mi and 56 mi, can not be consistent with the data; part of the winds exceed flight level winds.

4b. Two dimensional asymmetry

The boundary layer wind asymmetry due to the differential surface friction from storm motion is studied by (Chow 1971, Shapiro 1984) with the assumed circular pressure profile P(x) of Myers. The mean radial flow of the boundary layer determined by these models are sensitive to the boundary layer depth, h.

The surface wind analysis, based on many source of the real-time

data (from RECON, buoys, C-man stations), was produced by Hurricane Research Division (HRD). Fig. 10. showed a case comparison with HRD's analyzed winds at 1215Z, Oct. 4 (Houston, personal communication) vs. a parametric wind model (based only on central pressure, radius of maximum and storm motion) for hurricane Opal, 1995. They are similar in terms of a gross sense, but significant different in details. Using the same surge model, the maximum surges generated on the coast are comparable (Fig. 11). The contribution of pressure effect, vs. wind, is not negligible for this basin. However, the wind analysis at 1240Z (different data source), produced a less desirable answer.

This experiment seems to suggest that **the surge model is very conservative to small details of wind distribution.** The computed surge is more dependent the integral measure of the elements of TC, not its local perturbations.

5. Concluding Remark

The storm surge models respond to cyclones as meteorological systems in a very conservative manner, with respect to minor perturbations of the forcing. The extra-tropical storm surge prediction can directly link to the surface output from the NWP models and achieve improvements with the forcing. TC storm surge prediction, however, must continue to rely on a better engineering technique which requires certain degree of empiricism to account for current observations or/and dynamic constraints from TC models.

TC's track prediction is progressing rapidly, whereas the forecast of the intensity changes remains slow. This trend will continue, and limit the surge prediction capability to be as good as EC surge forecasts.

6. Reference

Atkinson, G. D., and C. R. Holliday, 1977: Tropical cyclone minimum sea level pressure maximum sustained wind relationship for the western North Pacific, Mon. Wea. Rev., 105,421-427.

Bunpagong, M., R. O. Reid, R. E. Whitaker, 1985: An investigation of hurricane-induced forerunner surge in the Gulf of Mexico, Tech. Report CERC-85-5, Dept. of Oceno., Taxas A&M, Taxas

Chen, Jye, W. A. Shaffer, and S. C. Kim, 1993: A forecast model for extratropical storm surge. Proceedings of the First International Conference on Hydro-Science and Engineering, Vol, Part b, Washington, D.C.

Chen, Jye, 1997: A comparison of two parametric wind models for hurricane storm surge prediction. (in press).

Emanuel, K. A., 1986: An air-sea interaction theory for tropical cyclones. Part I: Steady-State Maintenance, J. Atmos. Sci., 43, 585-604.

Holland, G. J., 1980: An analytic model of the wind and pressure profiles in hurricanes, Mon. Wea. Rev., 108,8,1212-1218.

Jelesnianski, C. P., 1966: Numerical computations of storm surges without bottom stress, Mon. Wea. Rev., 94, No. 6, 379-394.

Jelesnianski, C. P., and A. D. Taylor, 1973: A preliminary view of storm surges before and after storm modifications, NOAA Tech. Mem. ERL WMPO-3, NOAA, Dept. of Commerce, 33 pp.

Kim, Sung-Chan, Jye Chen, and W. A. Shaffer, 1996: An Operational Forecast Model for Extratropical Storm Surge along the U.S. East Coast, AMS Conf. on Coastal Oceanic and Atmospheric Prediction, Atlanta, GA, 1996, Jan. 28-Feb. 2.

Myers, V. A., 1954: Characteristics of United States hurricanes pertinent to levee design for Lake Okechobee, FL. Hydromet. Rep. 32, 126 pp.

Shaprio, L.J., 1983: The asymmetric boundary layer under a translating hurricane, J. Atmo. Sci., 40, 1984-1998.

Schloemer, R. W.,1954: Analysis and synthesis of hurricane wind patterns over Lake Okechobee, FL, Hydromet Rep. 31, 49 pp.

Qin, Z., 1993: Recent advances in storm surge prediction and research in China, In Tropical Cyclone Disasters, edited by J. Lighthill, Z. Zhemin, G. J. Holland, and K. A. Emanuel, Peking Univ. Press, Beijing, 423-441.

Ooyama, K., 1969: Numerical simulation of the life cycle of tropical cyclones, J. Atmos., Sci., 26, 3-40.

Weatherford, C., and W. M. Gray, 1988a: Typhoon structure as revealed by aircraft reconnaissance, Part I: Data analysis and climatology, Mon. Wea. Rev., 116, 1032-1043.

Weatherford, C., and W. M. Gray, 1988b: Typhoon structure as revealed by aircraft reconnaissance, Part II: Structural variability, Mon. Wea. Rev., 116, 1044-1056.

Willoughby, H. E., 1990b, Gradient balance in ropical cyclones, J. Atmos. Sci., 47, 265-274.

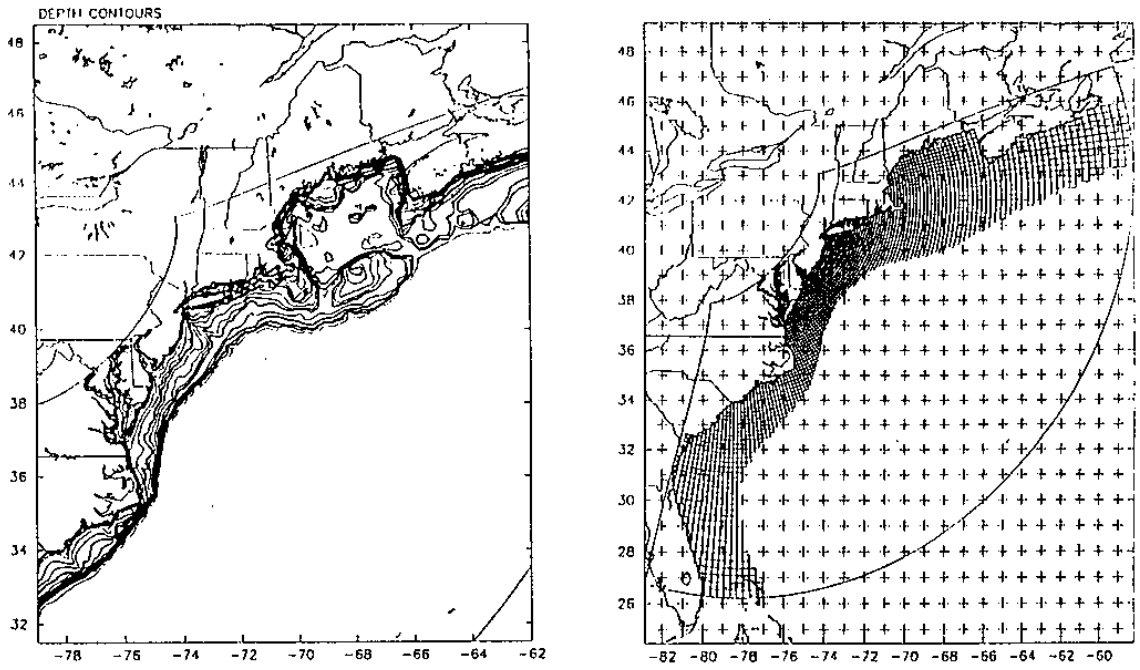

Fig. 1. EC grids and bathymetry for the East Coast of U.S.

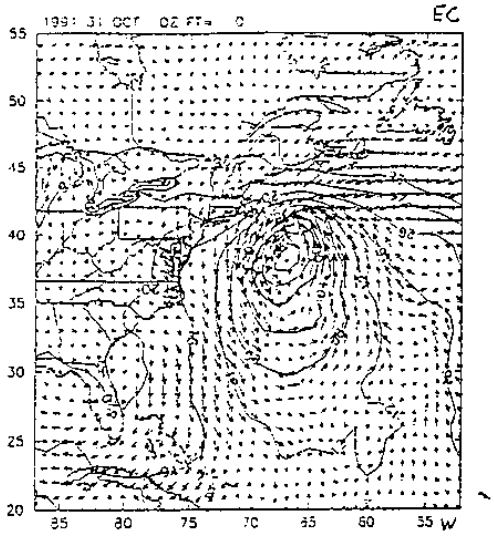

Fig. 2. Surface wind and pressure at 0000Z, Oct. 31, 1991 from AVN model.

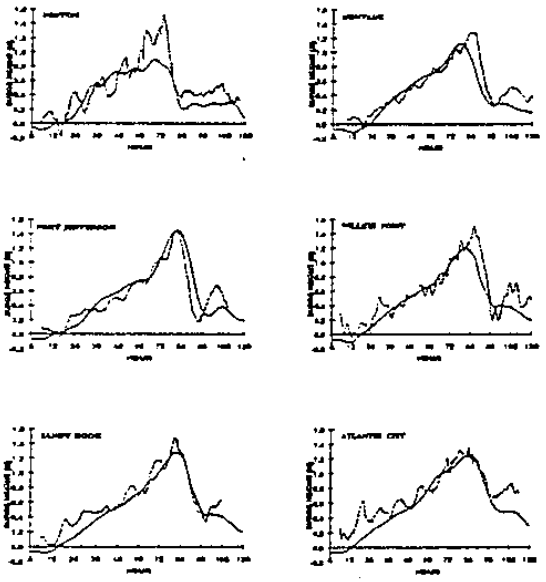

Fig. 3 Hindcast surge heights at six tide gages. The solid and dashed lines are for observations and model respectively.

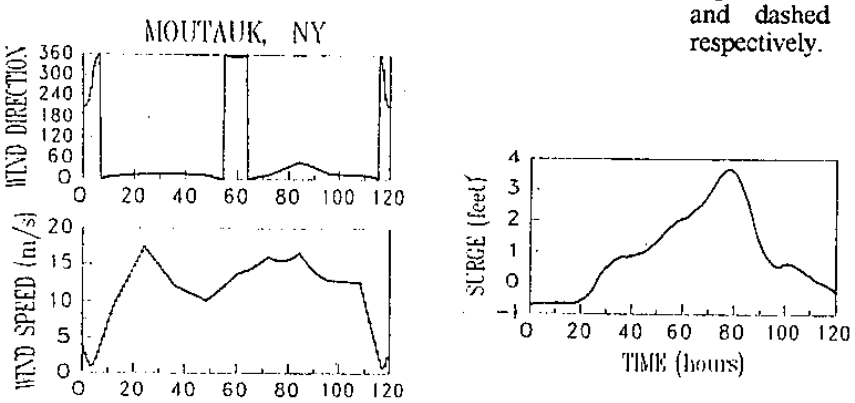

Fig. 4 Wind speeds and directions and hindasted surges at Montauk, NY.

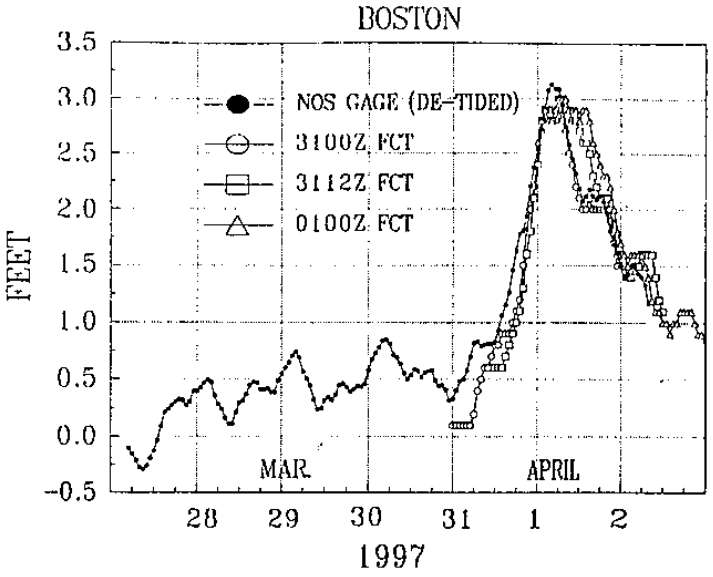

Fig. 5 The surge forecasts for three 12-hr forecast cycles at Boston, MA

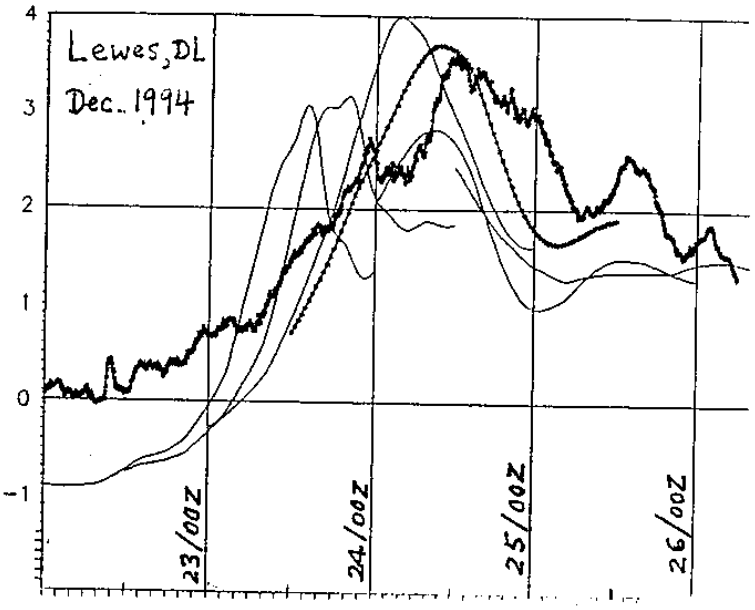

Fig. 6 The surge forecasts f or five 12-hr forecast cycles at Lewes, DL

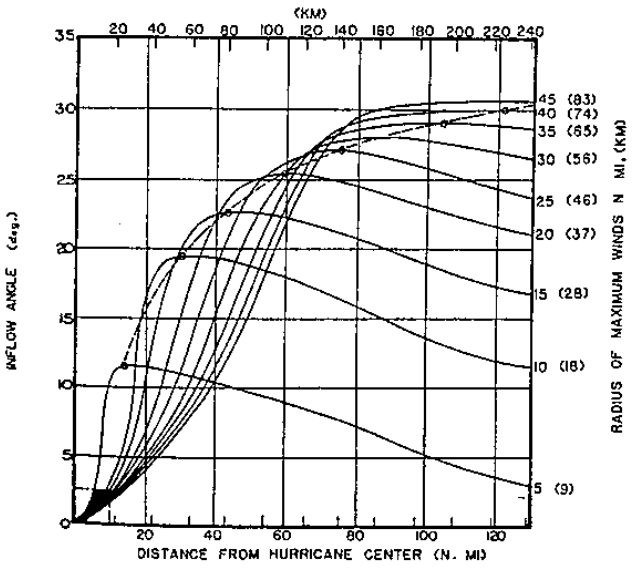

Fig. 7 Radial profiles of JT's inflow angle for different radius of maximum winds, R_m.

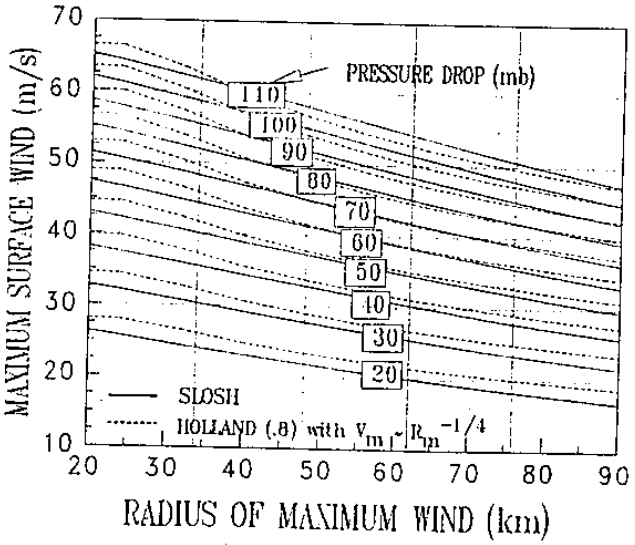

Fig. 8 Maximum surface winds vs. radius of maximum winds for different pressure drops.

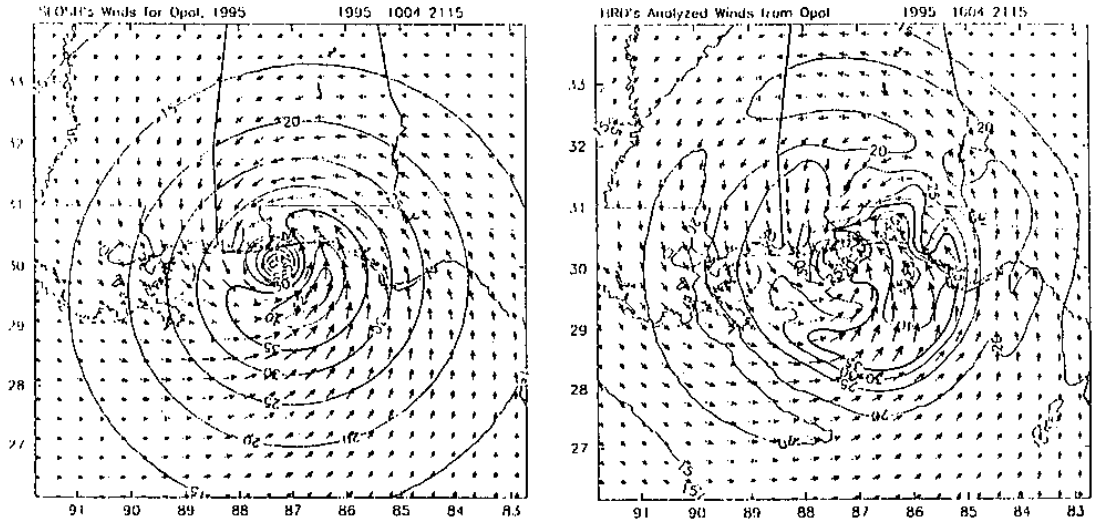

Fig. 9 SLOSH winds vs. HRD's analyzed surface winds for hurricane Opal, at 2115Z, Oct. 4 1995.

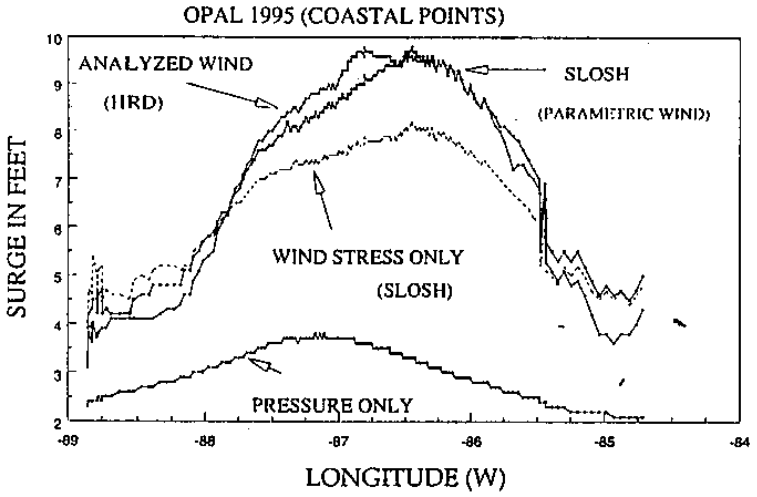

Fig. 10 Maximum surges for Opal winds from SLOSH and HRD analyzed.

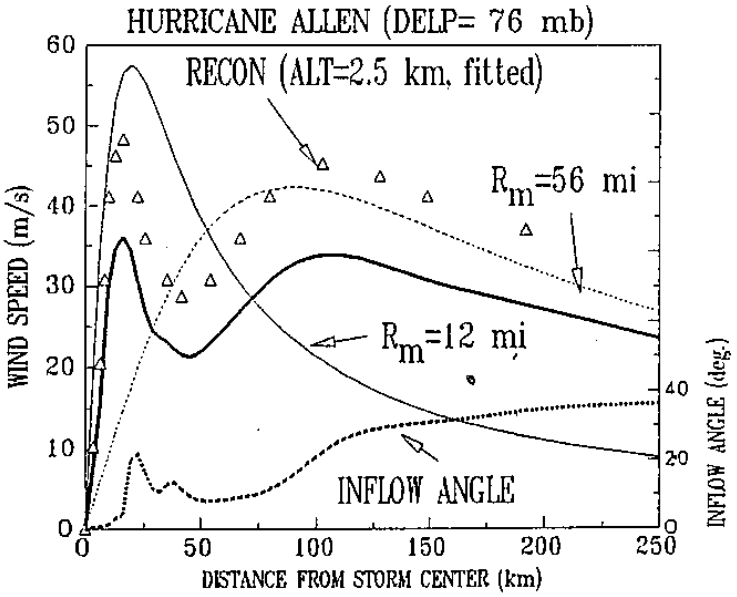

Fig. 11 Generalized SLOSH winds to fit RECON data from hurricane Allen, 1980, showing double wind maxima. and two single-peak profiles.